Zhongtang Huo
Jianqi Chen ✉
Lingjuan Hao
Jiansong Gao

https://doi.org/10.21278/TOF.492067324
ISSN 1333-1124
eISSN 1849-1391

AN ANALYSIS OF VIBRATION CHARACTERISTICS OF A ROTOR SYSTEM WITH COUPLING FAULTS OF BEARING LOOSENESS AND BEARING PEDESTAL LOOSENESS

Summary

Frequent disassembly of bearings leads to wear of the bearing pedestal hole, and a loose bearing impacts the bearing pedestal, causing it to loosen. To identify this type of malfunction, a dynamic model of the rotor system with the coupling faults of bearing looseness and bearing pedestal looseness was established based on the concentrated mass method of the rotor system. Also, the mapping relationship between the collision force and the vibration peak value was established and the coupling mechanism was described. The results indicate that when the coupling fault existed, the new frequency components were generated in the spectrum, and the frequency amplitude was positively correlated with the amount of looseness. Meanwhile, the increase in looseness would cause an increase in the amplitude of the fault characteristic frequency. Identifying the characteristic frequency and amplitude of looseness faults plays an important role in monitoring faults in rotor systems.

Key words: *bearing, pedestal, looseness, coupling, frequency*

1. Introduction

As a key component of the rotating equipment, the rotor system is widely used in precision machining, mining and metallurgy, transportation, wind power generation, and other fields [1-4]. As an important part, the operational status and fault characteristic recognition technology of the safe operation and maintenance of rotor systems has always been the focus of relevant studies [5-7]. Generally, the operational status of the rotor system can be determined by applying the frequency recognition technology, and this method usually requires dynamic models to be developed [8-11]. However, due to the occasional disassembly and assembly of bearings and manufacturing errors occurring from time to time, the wear of the bearing pedestal hole leads to the loosening of the bearing, which significantly reduces the operational accuracy and service life of the rotor system [12-14]. Wang [15] pointed out that bearing loose clearance and bearing clearance are typical nonlinear factors, and their existence leads to the nonlinearity of bearing vibration. Inagaki [16] explored nonlinear factors such as clearance and oil film between non-rotating and rotating components and obtained self-excited oscillation conditions for various nonlinear vibrations. He also studied the characteristics and mechanism of self-excited vibration. Shi [17] considered the bearing loosening problem caused by material in a system, described the outer ring motion as an independent model, and set temperature as an independent variable to describe the motion state of the outer ring. When the bearing is loose, it will constantly produce impact force on the bearing pedestal hole, and the vibration characteristics of the system will change. To solve the problem of anchor bolt looseness caused by bearing pedestal deformation, Guo [18] established a coupling dynamic model of the loosening-impact mode and analysed the reflection of the gap, eccentricity, etc. on the system's time-frequency spectrum. The research ideas provided great significance for fault diagnosis of a rotating subsystem.

Looseness faults will be reflected in the time-frequency characteristic curve of the rotor system, which is a rule summarised by many scholars [19-21]. Ma [22] established a support looseness model in which the anchor bolts were loose causing the bearing pedestal to loosen, and the relationship between the clearance and the system stiffness was obtained. However, since the gaps between the bearing and the bearing pedestal as well as between the bearing pedestal and the foundation cannot be ignored, the stiffness and damping of the system will be related to contact conditions, rather than always being the same value. Therefore, there are significant differences in the operating characteristics of the system. Thus, a more accurate dynamic response can be obtained [23, 24].

In the existing dynamic models of bearing looseness fault and pedestal looseness fault, the two faults were usually considered separately, without realizing that the bearing loosening fault might be the cause of the pedestal looseness fault. Furthermore, the pedestal looseness fault might cause the fault characteristics of the bearing looseness fault, thus ignoring the coupling effect between the two faults, which reduces the accuracy of fault monitoring. Therefore, in this paper, a dynamic model considering the coupling of the bearing i.e. bearing pedestal-foundation multiple looseness faults, was established, and the dynamic characteristics and the coupling mechanism of the system with the coupling of multiple looseness faults were discussed, which provided certain reference significance for ensuring the accuracy of condition monitoring of the rotor system. Section I introduces the topic of this paper; Section II describes the main steps of the model building; Section III and Section IV present the main results of the model and experimental validation, respectively.

2. Coupled dynamics modelling of multiple looseness faults

2.1 Loose bearing model

When a bearing runs in the worn pedestal, it will vibrate in the pedestal bore due to the excitation of the rotor. As shown in Fig. 1, after the bearing pedestal wears out, the bearing becomes loose, and the contact relationship between the bearing and the pedestal is equivalent to a contact pair composed of the spring-damping force.

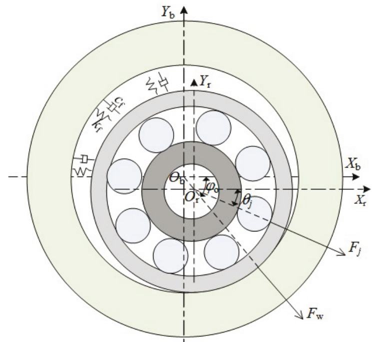

Fig. 1 Loose bearing model

For quantifying the movement of bearings, the bearing outer ring diameter is assumed to be d_0, and the bearing pedestal hole diameter is D_0. D_1 is the outer diameter of the bearing pedestal. Assuming that the wear of the bearing pedestal hole is uniform, that is, that there is no roundness and cylindricity error on the inner surface of the bearing pedestal, δ_f is defined as the amount of bearing loosening gap after the wear of the bearing pedestal. The mass of the bearing is m_r. $\{X_b, O_b, Y_b\}$ are defined as the position coordinate system of the bearing pedestal, and $\{X_r, O_r, Y_r\}$ as the motion coordinate system of the bearing. k_f, c_f represent the coefficient of the equivalent spring-damping contact pair between the bearing and the pedestal. F_j is the jth contact force due to the contact deformation between the rigid bodies. According to the force decomposition theory and Hertzian contact theory, the bearing support force can be expressed as [25]:

$$\begin{cases} F_x = \sum_{j=1}^{N_b} F_{jx} = \sum_{j=1}^{N_b} F_j \cos\theta_j \\ F_y = \sum_{j=1}^{N_b} F_{jy} = \sum_{j=1}^{N_b} F_j \sin\theta_j \end{cases} \tag{1}$$

where N_b represents the number of rolling elements in this type of bearing. Therefore, due to the mutual influence of vibration between the bearing and the bearing pedestal, the movement displacement of the bearing centre can be expressed as

$$e_0 = \sqrt{(x_r - x_b)^2 + (y_r - y_b)^2} \tag{2}$$

It can be concluded that the relationship between the motion angle positions of the bearing is:

$$\begin{cases} \sin\varphi_o = -\dfrac{x_r - x_b}{e_0} \\ \cos\varphi_o = -\dfrac{y_r - y_b}{e_0} \end{cases} \tag{3}$$

Considering the movement of the bearing and the bearing pedestal, the total deformation between the bearing and the bearing pedestal can be expressed as [26]:

$$\delta_w = (x_r - x_b)\cos\varphi_o + (y_r - y_b)\sin\varphi_o - \delta_f \tag{4}$$

Based on Hooke's law, F_w can be expressed as:

$$\begin{cases} F_w = k_f \delta_w^{1.5} & \delta_w > 0 \\ F_w = 0 & \delta_w \le 0 \end{cases} \tag{5}$$

Therefore, the component of the collision force F_W between the bearings in different directions can be expressed as:

$$\begin{cases} F_{wx} = F_w \cos\varphi_o \\ F_{wy} = F_w \sin\varphi_o \end{cases} \tag{6}$$

The manufacturing error is ignored, and wear occurs only on the inner surface of the bearing pedestal hole wall, and there is no wear on the outer surface of the bearing outer ring. When the radial movement of the bearing is less than the gap, the loose bearing and the bearing pedestal are not in contact, c_f, k_f are 0. When the bearing radial movement is greater than the gap, the outer ring will produce a collision force on the bearing pedestal, and it is considered that the spring-damping coefficients are both contact stiffness and equivalent damping. Therefore, c_f, k_f can be expressed as:

$$c_{\mathrm{f}} = \begin{cases} 0 & -\delta_{\mathrm{f}} \le e_0 \le \delta_{\mathrm{f}} \\ c_{\mathrm{f}}^{'} & else \end{cases} \tag{7}$$

$$k_{\mathrm{f}} = \begin{cases} 0 & -\delta_{\mathrm{f}} \le e_0 \le \delta_{\mathrm{f}} \\ k_{\mathrm{f}}^{'} & else \end{cases} \tag{8}$$

2.2 Bearing loosening-pedestal loosening coupling dynamics model

The bearing-shaft-pedestal system shown in Fig. 2 was set up, showing the positional relationship between bearings, bearing pedestals, foundation, and shaft to obtain a more realistic vibration response of multiple looseness coupling faults [27, 28]. The two bearings have the same model and rotate synchronously, letting the gap between the left-end bearing pedestal and the foundation be δ_{c1}.

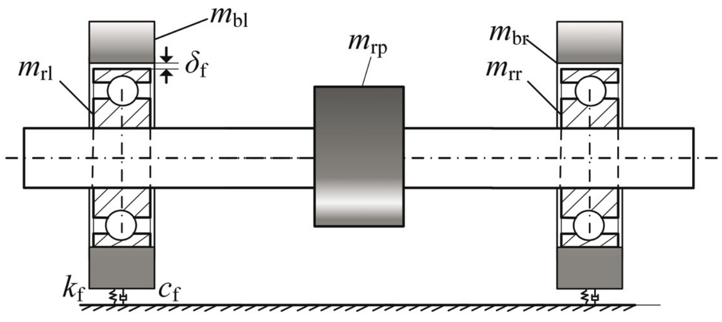

Fig. 2 Bearing-pedestal-foundation multi-loose coupling system

Gap δ_{c1} between the bearing pedestal and the foundation was added according to the concentrated mass law [29, 30]. At this point, the performance of the main components of the system is as follows: loose left-end bearing, fixed right-end bearing, loose left-end bearing pedestal, fixed right-end bearing pedestal, rotor disc vibration. The dynamic equation system can be expressed as:

$$m_{\mathrm{rp}}\ddot{x}_{\mathrm{rp}} + k(x_{\mathrm{rp}} - x_{\mathrm{rr}}) + k(x_{\mathrm{rp}} - x_{\mathrm{rl}}) + c(\dot{x}_{\mathrm{rp}} - \dot{x}_{\mathrm{rr}}) + c(\dot{x}_{\mathrm{rp}} - \dot{x}_{\mathrm{rl}}) = m_{\mathrm{rp}} e\omega^2 \cos\omega t \tag{9}$$

$$m_{\mathrm{rp}}\ddot{y}_{\mathrm{rp}} + k(y_{\mathrm{rp}} - y_{\mathrm{rr}}) + k(y_{\mathrm{rp}} - y_{\mathrm{rl}}) + c(\dot{y}_{\mathrm{rp}} - \dot{y}_{\mathrm{rr}}) + c(\dot{y}_{\mathrm{rp}} - \dot{y}_{\mathrm{rl}}) = m_{\mathrm{rp}} e\omega^2 \cos\omega t - m_{\mathrm{rp}}\mathrm{g} \tag{10}$$

$$m_{\mathrm{br}}\ddot{x}_{\mathrm{br}} + k_{\mathrm{cr}}x_{\mathrm{br}} + k_{\mathrm{fr}}(x_{\mathrm{br}} - x_{\mathrm{rr}}) + c_{\mathrm{cr}}\dot{x}_{\mathrm{br}} + c_{\mathrm{fr}}(\dot{x}_{\mathrm{br}} - \dot{x}_{\mathrm{rr}}) = -F_{x\mathrm{r}} \tag{11}$$

$$m_{\mathrm{br}}\ddot{y}_{\mathrm{br}} + k_{\mathrm{cr}}y_{\mathrm{br}} + k_{\mathrm{fr}}(y_{\mathrm{br}} - y_{\mathrm{rr}}) + c_{\mathrm{cr}}\dot{y}_{\mathrm{br}} + c_{\mathrm{fr}}(\dot{y}_{\mathrm{br}} - \dot{y}_{\mathrm{rr}}) = -F_{y\mathrm{r}} - m_{\mathrm{br}}\mathrm{g} \tag{12}$$

$$m_{\mathrm{bl}}\ddot{x}_{\mathrm{bl}} + k_{\mathrm{cl}}x_{\mathrm{bl}} + k_{\mathrm{fl}}(x_{\mathrm{bl}} - x_{\mathrm{rl}}) + c_{\mathrm{cl}}\dot{x}_{\mathrm{bl}} + c_{\mathrm{fl}}(\dot{x}_{\mathrm{bl}} - \dot{x}_{\mathrm{rl}}) = -F_{x\mathrm{l}} \tag{13}$$

$$m_{\mathrm{bl}}\ddot{y}_{\mathrm{bl}} + k_{\mathrm{cl}}y_{\mathrm{bl}} + k_{\mathrm{fl}}(y_{\mathrm{bl}} - y_{\mathrm{rl}}) + c_{\mathrm{cl}}\dot{y}_{\mathrm{bl}} + c_{\mathrm{fl}}(\dot{y}_{\mathrm{bl}} - \dot{y}_{\mathrm{rl}}) = -F_{y\mathrm{l}} - m_{\mathrm{bl}}\mathrm{g} - F_{\mathrm{b}} \tag{14}$$

$$m_{\mathrm{rr}}\ddot{x}_{\mathrm{rr}} + k_{\mathrm{fr}}(x_{\mathrm{rr}} - x_{\mathrm{br}}) + c_{\mathrm{fr}}(\dot{x}_{\mathrm{rr}} - \dot{x}_{\mathrm{br}}) + k(x_{\mathrm{rr}} - x_{r\mathrm{p}}) + c(\dot{x}_{\mathrm{rr}} - \dot{x}_{\mathrm{rp}}) = F_{x\mathrm{r}} \tag{15}$$

$$m_{\mathrm{rr}}\ddot{y}_{\mathrm{rr}} + k_{\mathrm{fr}}(y_{\mathrm{rr}} - y_{\mathrm{br}}) + c_{\mathrm{fr}}(\dot{y}_{\mathrm{rr}} - \dot{y}_{\mathrm{br}}) + k(y_{\mathrm{rr}} - y_{\mathrm{rp}}) + c(\dot{y}_{\mathrm{rr}} - \dot{y}_{\mathrm{rp}}) = F_{y\mathrm{r}} - m_{\mathrm{rr}}\mathrm{g} \tag{16}$$

$$m_{\mathrm{rl}}\ddot{x}_{\mathrm{rl}} + k_{\mathrm{fl}}(x_{\mathrm{rl}} - x_{\mathrm{bl}}) + c_{\mathrm{fl}}(\dot{x}_{\mathrm{rl}} - \dot{x}_{\mathrm{bl}}) + k(x_{\mathrm{rl}} - x_{\mathrm{rp}}) + c(\dot{x}_{\mathrm{rl}} - \dot{x}_{\mathrm{rp}}) = F_{x\mathrm{l}} \tag{17}$$

$$m_{\mathrm{rl}}\ddot{y}_{\mathrm{rl}} + k_{\mathrm{fl}}(y_{\mathrm{rl}} - y_{\mathrm{bl}}) + c_{\mathrm{fl}}(\dot{y}_{\mathrm{rl}} - \dot{y}_{\mathrm{bl}}) + k(y_{\mathrm{rl}} - y_{\mathrm{rp}}) + c(\dot{y}_{\mathrm{rl}} - \dot{y}_{\mathrm{rp}}) = F_{y\mathrm{l}} - m_{\mathrm{rl}}\mathrm{g} \tag{18}$$

In the above model, the mass of the shaft is assumed to be m_{rp}, and the mass is assumed to be concentrated on the disk. m_{rl} and m_{rr} are the masses of two identical bearings; m_{bl} and m_{br} are the masses of the same type of bearing pedestals in the system; e is the eccentricity. Let the impact between the bearing pedestal and the foundation be F_b, then this force is related to the bearing support force and the impact force between the bearing and the bearing pedestal, that is:

$$F_{\mathrm{b}} = F_y - F_{\mathrm{w}y} \tag{19}$$

When the bearing pedestal leaves the foundation, there are two types of looseness faults in the system: loose bearing and loose bearing pedestal. Fig. 3 shows that the bearing loosening and the bearing pedestal loosening occur simultaneously in the system.

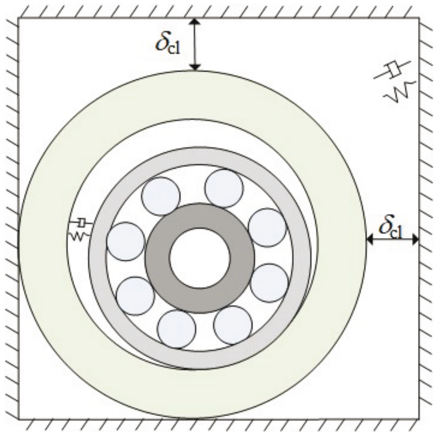

Fig. 3 Model with gaps between bearing and bearing pedestal as well as between bearing pedestal and foundation

Therefore, according to the rigid body contact situation and the stiffness-damping coefficient relationship, the stiffness and damping between the foundation and the left-end bearing pedestal, respectively, are represented as:

$$c_{\mathrm{cl}} = \begin{cases} c_{\mathrm{cl}}^{'} & else \\ 0 & 0 \le y_{\mathrm{bl}} \le \delta_{\mathrm{cl}} \end{cases} \tag{20}$$

$$k_{\mathrm{cl}} = \begin{cases} k_{\mathrm{cl}}^{'} & else \\ 0 & 0 \le y_{\mathrm{bl}} \le \delta_{\mathrm{cl}} \end{cases} \tag{21}$$

3. Simulation and analysis of a multi-looseness coupled dynamics model

To study the coupling principle of various looseness faults in a multi-loosening model and vibration characteristics at locations where multiple looseness faults occur, the simulation calculation first simulates the situation with only bearing looseness fault and then adds a 0.1 mm gap between the bearing pedestal and the foundation to simulate the dynamic response of the system when two faults exist. The selected bearing model is JIS6306 when there is no looseness fault in the system, the damping coefficient is 2,100 N·s/m, and the contact stiffness is 2.5×10^8 N/m. Assuming δ_f =0.1 mm, the system speed is 1,980 r/min, and both m_{br} and m_{bl} are 4.6 kg. The partial dimensions of the bearing and the bearing pedestal are listed in Table 1, mainly including the structural parameters.

Table 1 Dimensions of bearing and pedestal

Name	Value
Outer ring inner raceway radius (mm)	31.95
Rolling element number	8
Inner ring outer raceway radius (mm)	20.05
Outer diameter of pedestal (mm)	170
Bearing clearance (mm)	0.005

3.1 Bearing looseness fault

According to the parameter requirements of the simulation settings, the mass of the rotor disc is about 9 kg, the mass of the two bearings is about 2 kg, and the time step of the simulation calculation is 10^{-5}. The vibration curve of the bearing with the looseness fault at the left end is shown in Fig. 4.

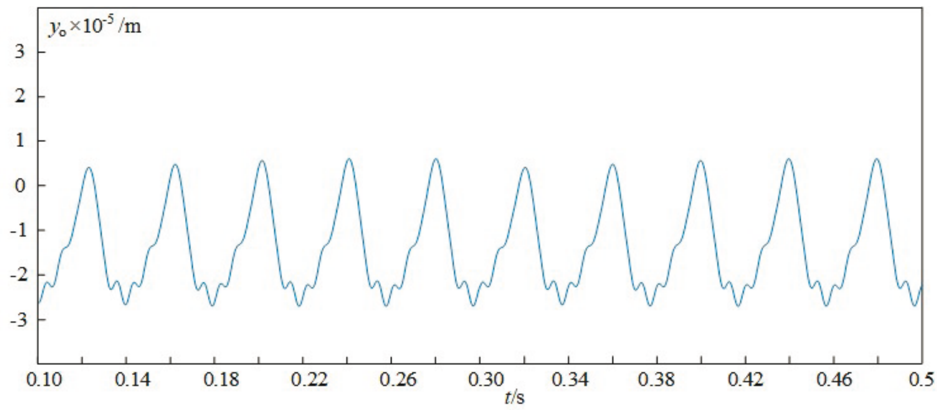

Fig. 4 Bearing looseness displacement

As shown in Fig. 4, the loose bearing presents an uneven distribution of vibration displacement in the vertical direction. The main manifestation is that the negative half-axis vibration displacement of y is large, and the positive half-axis vibration displacement of y is small. This is mainly because the centrifugal force provided by the system and the impact force are not enough to overcome the gravity and load, and the loose bearing has a smaller range of trajectory in the bearing bore and cannot reach the top of the bearing bore. The numerical results are transformed by the Fast Fourier Transform (FFT) to obtain the frequency representation of the loose bearing, and the spectrum is shown in Fig. 5.

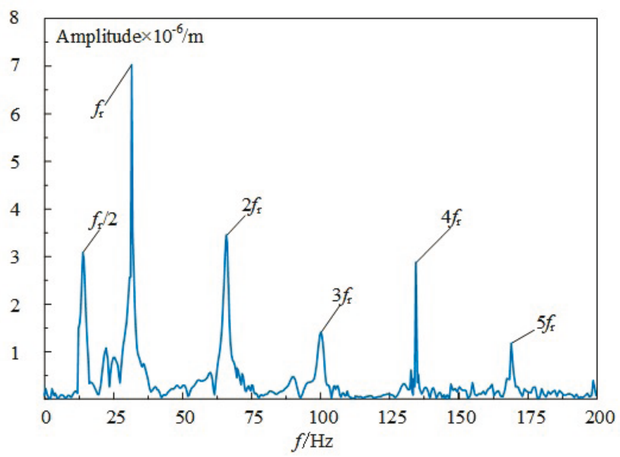

Fig. 5 FFT spectrum of bearing looseness

The vibration spectrum containing the looseness fault is shown in Fig. 5, where the main components are f_r and its octave components. At the same time, $f_r/2$ appears in the spectrum as a characteristic of the rotor system touch-friction fault, indicating that the bearing and pedestal had a touch-friction effect. In addition, the amplitude of f_r is the highest in the spectrum, which indicates that the contribution of the looseness fault to the spectrum is smaller than the rotation frequency at this time, but it is still possible to judge the bearing looseness fault by the appearance of $f_r/2$.

3.2 Loose bearing-pedestal coupling fault

To distinguish between the response to bearing looseness fault and the response to bearing pedestal looseness fault, the fault response of bearing pedestal looseness is obtained after bearing looseness occurs and a gap of 0.1 mm between the bearing and the bearing pedestal is maintained, as well as between the bearing pedestal and the foundation. In the rotor system shown in Fig. 2, the left-end bearing is loose and the left-end bearing pedestal is loose; the right-end bearing is fixed and the right-end bearing pedestal is fixed. By solving the dynamic model again, the response of the left-end bearing pedestal under the above conditions was obtained as shown in Fig. 6.

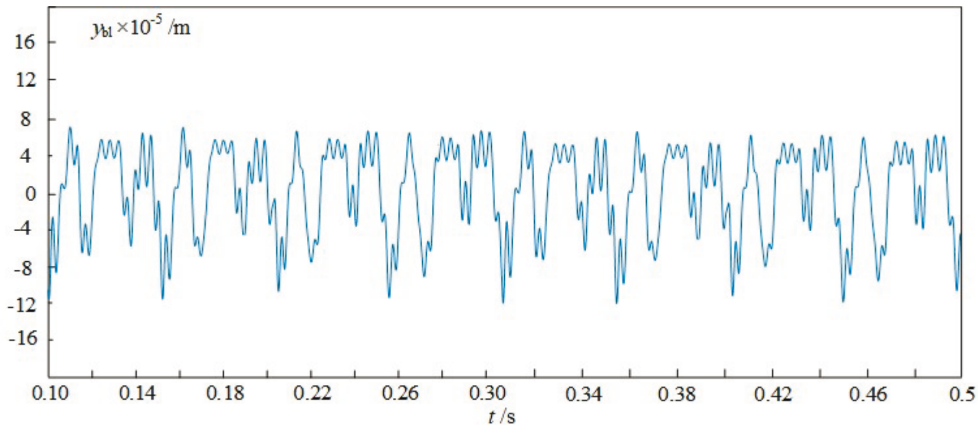

Fig. 6 Time domain of left-end bearing pedestal

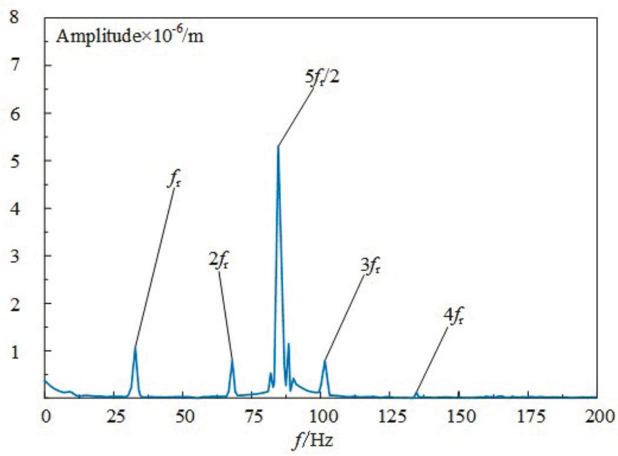

Fig. 7 Fast Fourier transform result of Fig. 6

As shown in Figs. 6 and 7, the bearing pedestal vibrated due to the amount of looseness between the foundation and the left-end bearing pedestal. Similarly to the vibration as shown in Fig. 4, the reason for the vibration of the bearing pedestal in the *y*-axis is that the impact of the bearing on the bearing pedestal is greater than the gravity of the bearing pedestal. This impact force is opposite to the gravity of the bearing pedestal, the distance the bearing pedestal moves upwards depends on the difference between the instantaneous impact force and gravity. The curve located on the y-negative half-axis is derived from the fact that the impact force of the bearing on the bearing pedestal is consistent with the direction of gravity. The reason for the significant negative vibration of the bearing pedestal is that the displacement at this time depends on the sum of the gravity and the impact force. Therefore, the amplitude of the negative y-axis is greater than that of the positive y-axis.

In addition, a new frequency component $5f_r/2$ appeared in the spectrum in addition to f_r and its octave components, and the amplitude of $5f_r/2$ is the highest in the spectrum at this time, which can be considered as the characteristic frequency of the bearing pedestal looseness based on the experience presented in a previous study [11]. At the same time, because f_r and its octave components are mainly related to the rotation of the rigid body and the bearing pedestal does not rotate with the rotor's rotation, the appearance of f_r and its octave components in the spectrum is due to the bearing rotation frequency caused by eccentric excitation, which is transmitted to the bearing pedestal vibration through the bearing. However, due to vibration attenuation, their amplitude is less than $5f_r/2$'s.

To further explain the coupling mechanism of bearing loosening and bearing pedestal loosening, the collision force and the support force between the bearing and the bearing pedestal were compared and analysed by calculating the dynamic model of the bearing at multiple loose positions. Also, the collision force between the bearing and the bearing pedestal, the bearing force, the impact force between the bearing pedestal and the foundation, and the impact on the vibration waveform were described, revealing the reasons for waveform changes. The overall relationship diagram is shown in Fig. 8.

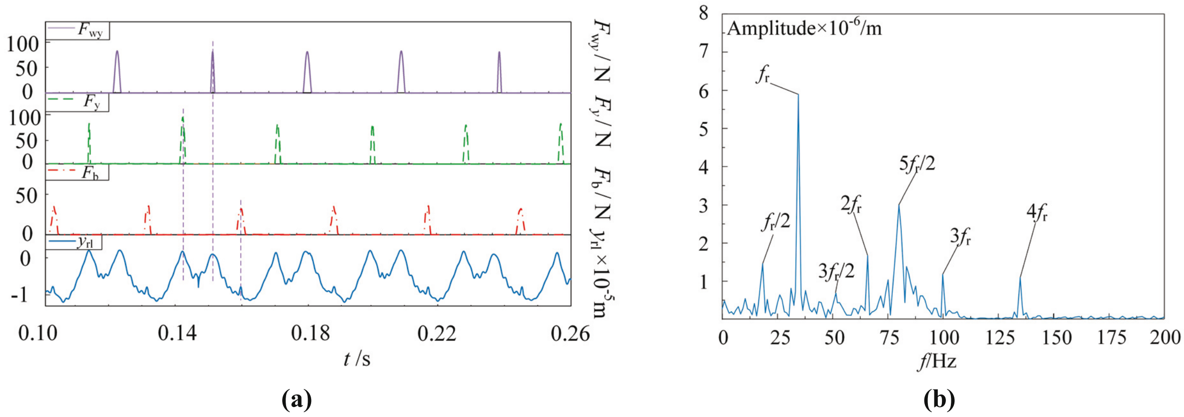

Fig. 8 (a) Influence of various forces on waveform (b) Frequency spectrum of left-end bearing vibration

Collision force F_{wy}, supporting force F_y, and collision force F_b between the foundation and the loose bearing pedestal correspond to major wave peaks in the vibration curve of the left-end bearing as shown in Fig. 8(a), revealing the cause of fluctuations in the time-domain waveform, i.e. these forces are the cause of the curve fluctuations. In addition, the vibrations of the bearing pedestal and the bearing restrict and affect each other after the bearing pedestal is loosened, and the realization form is that the moving boundary of the loose bearing changes, resulting in a decrease in amplitude.

Compared with Fig. 7, more frequency components appear in the spectrum of Fig. 8 (b), among which $3f_r/2$ is more obvious. However, when a bearing looseness fault occurs, the spectrum shows an increase in the $f_r/2$ amplitude, and $5f_r/2$ is the frequency representation of the bearing pedestal looseness after multiple looseness occurrences. Both of them are reflected in the spectrum, so it can be inferred that $3f_r/2$ is the characteristic frequency of the coupled fault after the two types of faults occur simultaneously.

3.3 Effect of gap coupling fault characteristics

3.3.1 Influence of bearing pedestal gap on coupling fault characteristics

As shown in Fig. 9, the initial value is changed, the gap between the bearing pedestal and the foundation is set to be 0.1 mm, 0.2 mm, 0.3 mm, and 0.4 mm, and the vibration spectrum of the bearing is calculated in the *y*-direction.

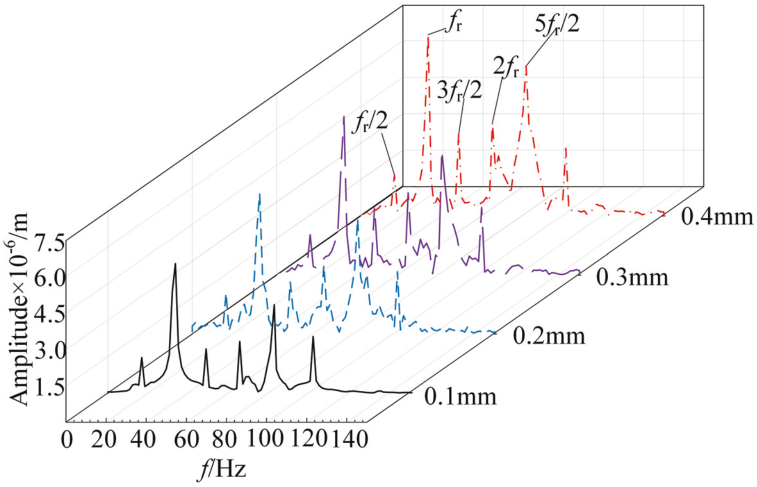

Fig. 9 Bearing vibration spectrum for different amounts of pedestal looseness

With the loosening between the foundation and the bearing pedestal increasing, the main frequency in the bearing vibration spectrum of the bearing is still f_r and its octave, manifested as the rotational frequency amplitude, is always the greatest. At the same time, the $5f_r/2$ and $3f_r/2$ amplitudes increase, but the $f_r/2$ amplitude barely changes.

This is because the increase in the amount of bearing pedestal looseness leads to the intensification of collisions between the bearing pedestal and the foundation, causing the amplitude of the characteristic frequency $5f_r/2$ (for bearing pedestal looseness faults) to increase; and $f_r/2$ is mainly associated with bearing looseness, although the amount of bearing pedestal looseness leads to the vibration boundaries changing, affecting the bearing's trajectory, but the amount of bearing looseness does not occur in addition to the elasticity of the deformation of the growth, so in the case of the $f_r/2$ amplitude there is not a large difference. Also, from the above-presented data, when it comes to the coupling effect of the two kinds of faults, it appears that there is a large increase in the amplitude of the coupling fault frequency $3f_r/2$.

3.3.2 Influence of bearing gap on coupling fault characteristics

As shown in Fig. 10, the initial value is changed in the simulation, the gap between the bearing and the foundation is set to be 0.1 mm, 0.2 mm, 0.3 mm, and 0.4 mm, and the vibration spectrum is calculated in the vertical direction.

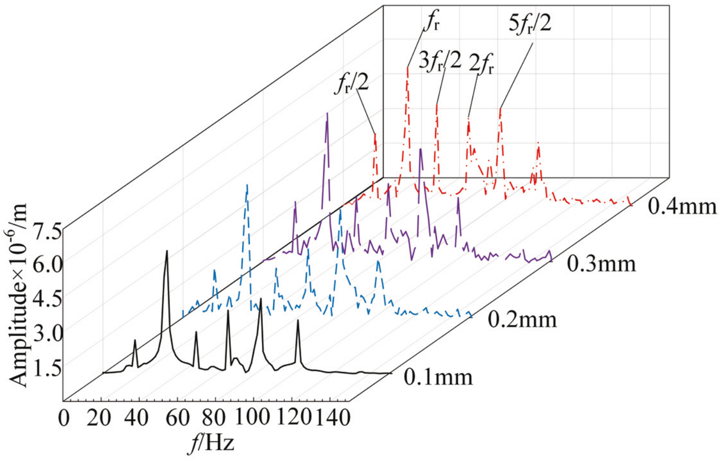

Fig. 10 Vibration spectrum of bearing with different bearing looseness amount

Although the bearing looseness increases, the main frequency component of the bearing vibration spectrum is still f_r and its harmonic components, which shows that the rotation frequency amplitude is always the greatest. At the same time, the $f_r/2$, and $3f_r/2$ values increase, but $5f_r/2$ values barely change. This is because the increase in bearing looseness leads to the intensification of collisions between the bearing pedestal and the bearing, causing the amplitude of the characteristic frequency fr/2 for bearing looseness faults to increase. $5f_r/2$ is mainly related to the looseness of the bearing pedestal. Although the change of the bearing looseness changes the vibration boundary of the system and affects the movement trajectory of the bearing pedestal, the main contribution to the variation of the gap between the foundation and the bearing pedestal still comes from a negligible elastic deformation, so the $5f_r/2$ amplitude has no great difference. Then, from the data presented above, in the coupling effect of the two kinds of faults, the amplitude of the coupling fault frequency $3f_r/2$ significantly increases.

4. Experimental verification

To investigate the characteristic frequency of multiple looseness faults in the rotor system and to test the correctness of the model presented in this paper, an experimental program was established and the model was validated on a rotor experimental bench. The experimental facility is shown in Fig. 11.

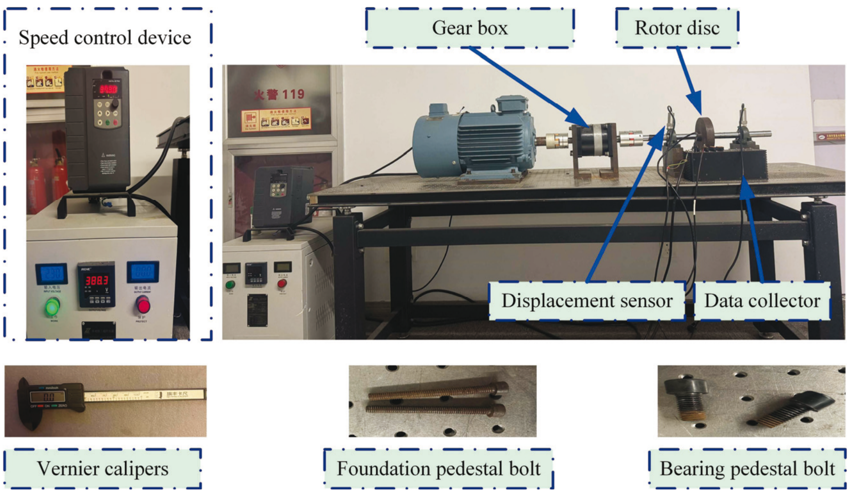

Fig. 11 Coupling fault verification test bed

As can be seen in Fig. 11, the speed is controlled by a speed controller. The output speed of the motor ranges from 0 to 10,000 r/min, and the output is stable. The bearing model selected in the experiment is the same as the simulation calculation, as shown in Table 1. The y-displacement signal is collected by a contact displacement sensor at the sampling frequency of 1,024 Hz and collected by a data collector.

The bearing pedestal hole was polished with sandpaper, during which the circumference size was measured by a vernier caliper and a roundness meter many times so that the gap between the bearing pedestal and the bearing was 0.1 mm, 0.2 mm, 0.3 mm, and 0.4 mm, and the arc degree of the bearing pedestal hole was ensured. To ensure that the gap between the foundation and the bearing pedestal was consistent with the simulation, a vernier caliper was used to measure the screw length of the anchor bolt of the bearing pedestal and the screw hole length of the anchor bolt, and the screw length was controlled so that the gap between the foundation and the bearing pedestal was 0.1mm, 0.2mm, 0.3mm, and 0.4mm.

First, the speed of the rotor was 1,980 r/min and the mass of the rotor disc in the middle position of the shaft was 9 kg, so that the gap between the bearing pedestal and the bearing was 0.1 mm, 0.2 mm, 0.3 mm, and 0.4 mm, the gap between the foundation and the bearing pedestal was 0.1mm, and the spectrum of the multi-loosening coupled rotor system was computed, as shown in Fig. 12. The results showed that the amplitude of the bearing looseness fault characteristic $f_r/2$ and the amplitude of the coupling fault characteristic $3f_r/2$ increased with the gap expansion, while the amplitude of $5f_r/2$ remained almost unchanged. This indicates that the bearing looseness aggravates the coupling fault characteristics but has a negligible influence on the bearing pedestal looseness fault, which is confirmed by the simulation analysis in Section 3.

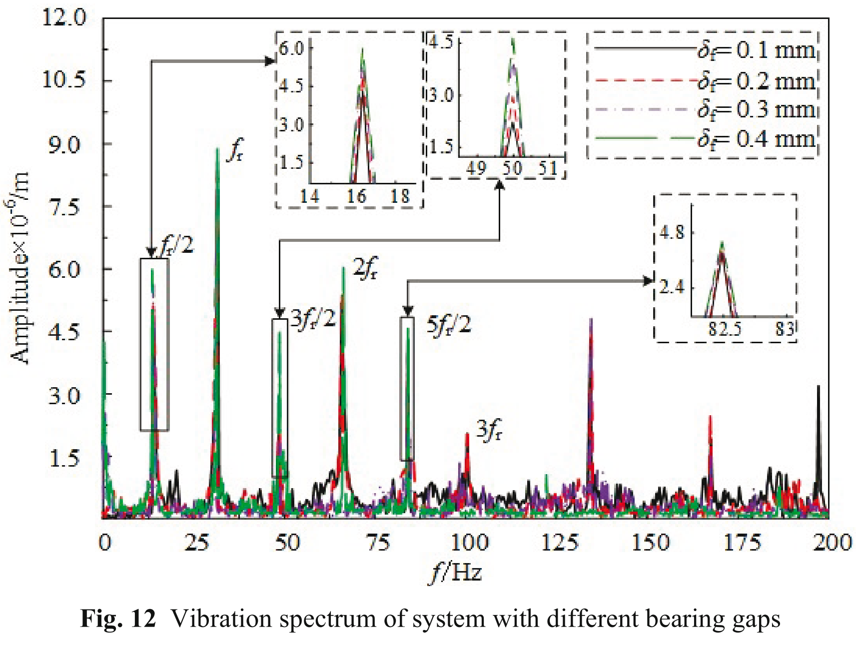

Fig. 12 Vibration spectrum of system with different bearing gaps

As shown in Fig. 13, by setting the system speed to 1,980 r/min so that the gap between the foundation and the bearing pedestal was 0.1 mm, 0.2 mm, 0.3 mm, and 0.4 mm, and the bearing gap was 0.1 mm, the spectrum of the multi-loosening coupled system was obtained. The results showed that the $5f_r/2$ amplitude of the bearing pedestal looseness fault characteristic, the coupling fault characteristic $3f_r/2$ amplitude increased with the gap, but the $f_r/2$ amplitude related to the bearing looseness fault characteristic was almost unchanged, indicating that the bearing pedestal looseness exacerbates the coupling fault characteristic, and the influence on the bearing looseness fault can be ignored, which was confirmed by the simulation analysis in Section 3.

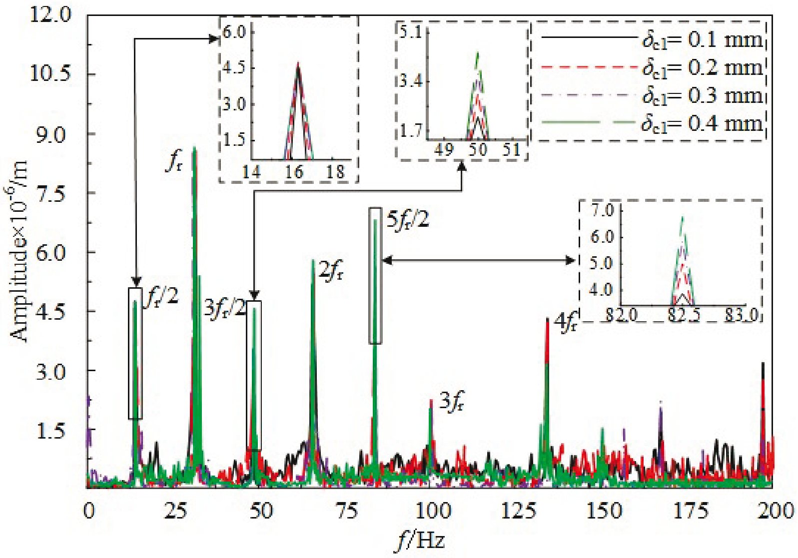

Fig. 13 Vibration spectrum of system with different bearing pedestal gaps

5. Conclusion

In this paper, the multi-loosening coupling dynamics model of bearing looseness and pedestal looseness was established, and the coupling mechanism and characteristic frequency of bearing looseness and pedestal looseness were explored. The main conclusions of the study are as follows.

(1) When bearing looseness fault occurs, the fault characteristic frequency is mainly $f_r/2$; when bearing pedestal looseness fault occurs, the fault characteristic frequency is mainly $5f_r/2$.

(2) When both bearing looseness and pedestal looseness faults occur at the same time, changing the degree of one fault has little impact on the characteristics of the other fault.

(3) The mutual influence between the bearing looseness faults and the pedestal looseness faults is mainly manifested by the impact force at different locations leading to the appearance of wave peaks related to the impact force on the vibration time domain, and the coupled fault frequency is $3f_r/2$ components. The results of the study provide a theoretical basis for a fault diagnosis of coupled multiple looseness faults of a rotor system.

REFERENCES

[1] Shi H, Bai X, Zhang K, et al. Effect of thermal-related fit clearance between outer ring and pedestal on the vibration of full ceramic ball bearing. Shock and Vibration, 2019, 2019. https://doi.org/10.1155/2019/8357807

[2] Wang P, Xu H, Yang Y, et al. Dynamic characteristics of ball bearing-coupling-rotor system with angular misalignment fault. Nonlinear Dynamics, 2022, 108(4): 3391-3415. https://doi.org/10.1007/s11071-022-07451-1

[3] Zhang J, Zhang Y, Zhou E, et al. Research on multi-body dynamic model of automatic discrete system for protection bearing without cage. Nonlinear Dynamics, 2023, 111(22): 20869-20897. https://doi.org/10.1007/s11071-023-08904-x

[4] Tian M, Su X, Chen C, et al. Bearing fault diagnosis of wind turbines based on dynamic multi-adversarial adaptive network. Journal of Mechanical Science and Technology, 2023, 37(4): 1637-1651. https://doi.org/10.1007/s12206-023-0306-z

[5] Da Silva Tuckmantel F W, Cavalca K L. Vibration signatures of a rotor-coupling-bearing system under angular misalignment. Mechanism and Machine Theory, 2019, 133: 559-583. https://doi.org/10.1016/j.mechmachtheory.2018.12.014

[6] Wang, P., Xu, H., Ma, H., et al. Nonlinear response of rotor system with bearing dynamic misalignment. Mechanics Based Design of Structures and Machines, 2023, 52(5), 2532–2553. https://doi.org/10.1080/15397734.2023.2185634

[7] Deng S, Zhao C, Hua L, et al. Dynamic behaviors of angular contact ball bearings based on nonlinear dynamic model with flexible ring and cage motion whirl. Nonlinear Dynamics, 2023, 111(12): 10879-10909. https://doi.org/10.1007/s11071-023-08412-y

[8] Xu H, Wang P, Ma H, et al. Analysis of axial and overturning ultimate load-bearing capacities of deep groove ball bearings under combined loads and arbitrary rotation speed. Mechanism and Machine Theory, 2022, 169. https://doi.org/10.1016/j.mechmachtheory.2021.104665

[9] Xu H, Ren H, Qin D. Dynamic characteristics of the planetary gear system with rolling bearing. Multibody System Dynamics, 2023, 59(2): 171-191. https://doi.org/10.1007/s11044-023-09905-9

[10] Yang C, Wu X, Chi M, et al. A modelling methodology of the axle box bearing-vehicle coupled system dynamics. Vehicle System Dynamics, 2023: 1-23. https://doi.org/10.1080/00423114.2023.2235031

[11] Hemati A, Shooshtari A. Bearing Failure Analysis Using Vibration Analysis and Natural Frequency Excitation. Journal of Failure Analysis and Prevention, 2023, 23(4): 1431-1437. https://doi.org/10.1007/s11668-023-01700-0

[12] Wang H F, Chen G, Song P P. Asynchronous vibration response characteristics of aero-engine with support looseness fault. Journal of Computational and Nonlinear Dynamics, 2016, 11(3): 031013. https://doi.org/10.1115/1.4031245

[13] Wang H F, Chen G. Certain type turbofan engine whole vibration model with support looseness fault and casing response characteristics. Shock and Vibration, 2014, 2014. https://doi.org/10.1155/2014/683469

[14] Ma S, Li W, Yan K, et al. A study on the dynamic contact feature of four-contact-point ball bearing. Mechanical systems and signal processing, 2022, 174. https://doi.org/10.1016/j.ymssp.2022.109111

[15] Wang H, Chen G, Song P. Asynchronous vibration response characteristics of connectors with looseness fault and its verification. Journal of Vibroengineering, 2015, 17(7): 3551-3560.

[16] Inagaki M, Ishida Y. Mechanism of occurrence of self-excited oscillations of a rotor with a clearance between bearing holder and housing[C]//International Design Engineering Technical Conferences and Computers and Information in Engineering Conference. 2011, 54785: 965-974. https://doi.org/10.1115/DETC2011-48052

[17] Shi H, Li Y, Bai X, et al. Investigation of the orbit-spinning behaviors of the outer ring in a full ceramic ball bearing-steel pedestal system in wide temperature ranges. Mechanical Systems and Signal Processing, 2021, 149. https://doi.org/10.1016/j.ymssp.2020.107317

[18] Nan G, Yao J, Chen X, et al. Coupling dynamics of pedestal looseness and impact-rub for rotor system with nonlinear support. Advances in Mechanical Engineering, 2024, 16(1). https://doi.org/10.1177/16878132231222907

[19] Bai X, Sun M, Wang Z, et al. Loose Coupling Mechanism and Fault Characteristics Analysis of Multiple Connections in Full Ceramic Bearing-Pedestal-Foundation System Within Wide Temperature Ranges. Journal of Failure Analysis and Prevention, 2024: 1-13. https://doi.org/10.1007/s11668-024-01862-5

[20] Chu F, Tang Y. Stability and non-linear responses of a rotor-bearing system with pedestal looseness. Journal of Sound and Vibration, 2001, 241(5): 879-893. https://doi.org/10.1006/jsvi.2000.3341

[21] He Y, Chen Z, Guo D, et al. A genetic algorithm based inverse problem approach for pedestal looseness identification in rotor-bearing systems. Key Engineering Materials, 2003, 245-246: 115-122. https://doi.org/10.4028/www.scientific.net/KEM.245-246.115

[22] Ma H, Zhao X, Teng Y, et al. Analysis of dynamic characteristics for a rotor system with pedestal looseness. Shock and vibration, 2011, 18(1-2): 13-27. https://doi.org/10.1155/2011/753047

[23] Jin Y, Liu Z, Yang Y, et al. Nonlinear vibrations of a dual-rotor-bearing-coupling misalignment system with blade-casing rubbing. Journal of Sound and Vibration, 2021, 497. https://doi.org/10.1016/j.jsv.2021.115948

[24] Kato M, Kono D, Kakinuma Y. Dynamical characteristic validation of motorized CFRP spindle unit based on receptance coupling. Mechanical Systems and Signal Processing, 2022, 173. https://doi.org/10.1016/j.ymssp.2022.109028

[25] Li Y, Li Z, He D, et al. Nonlinear dynamic characteristics of rolling bearings with multiple defects. Journal of Vibration Engineering & Technologies, 2023, 11(8): 4303-4321. https://doi.org/10.1007/s42417-022-00816-1

[26] Sawalhi N, Randall R B. Simulating gear and bearing interactions in the presence of faults: Part I. The combined gear bearing dynamic model and the simulation of localised bearing faults. Mechanical Systems and Signal Processing, 2008, 22(8): 1924-1951. https://doi.org/10.1016/j.ymssp.2007.12.001

[27] Bai X, Zheng H, Wang Z, et al. Investigation on the misalignment of full ceramic ball bearing rotor system caused by varying gap in wide temperature ranges. Proceedings of the Institution of Mechanical Engineers, Part C: Journal of Mechanical Engineering Science, 2022. https://doi.org/10.1177/09544062221132184

[28] Cao Z, Wu G, He C, et al. A new instantaneous contact based dynamic model of rolling element bearings with local defects. Mechanical Systems and Signal Processing, 2023, 200. https://doi.org/10.1016/j.ymssp.2023.110600

[29] Ma Q, Liu Y, Yang S, et al. A coupling model of high-speed train-axle box bearing and the vibration characteristics of bearing with defects under wheel rail excitation. Machines, 2022, 10(11): 1024. https://doi.org/10.3390/machines10111024

[30] Wang H. A modeling method for a rotor system with an active floating ring squeeze film damper. Proceedings of the Institution of Mechanical Engineers, Part C: Journal of Mechanical Engineering Science, 2021, 235(4): 627-638. https://doi.org/10.1177/0954406220939112

Submitted: 30.4.2024
Accepted: 22.10.2024

Assist. Prof. Zhongtang Huo
Dr. Jianqi Chen*
Dr. Lingjuan Hao
Dr. Jiansong Gao
Mechanical and Electrical College,
Handan University, Hanshan District,
Handan City, Hebei, China
*Corresponding author:
chenjianqi1106@163.com